2002

A Dynamic Model Of A Vapor Compression Liquid Chiller

S. Bendapudi
Purdue University

J. E. Braun
Purdue University

E. A. Groll
Purdue University

A DYNAMIC MODEL OF A VAPOR COMPRESSION LIQUID CHILLER

Satyam Bendapudi, 1077 Ray W. Herrick Laboratories, School of Mech. Eng.,
Purdue University, West Lafayette, IN 47906, USA
Phone: (765) 494-2147; Fax: (765) 494-0787
Email: satyam@purdue.edu *Author for correspondence

James E. Braun, PhD., 1077 Ray W. Herrick Laboratories, School of Mech. Eng.,
Purdue University, West Lafayette, IN 47906, USA
Phone: (765) 494-9157; Fax: (765) 494-0787
Email: jbraun@ecn.purdue.edu

Eckhard A. Groll, PhD., 1077 Ray W. Herrick Laboratories, School of Mech. Eng.,
Purdue University, West Lafayette, IN 47906, USA
Phone: (765) 496-2201; Fax: (765) 494-0787
Email: groll@ecn.purdue.edu

ABSTRACT

Dynamic models of vapor compression systems are important tools for HVAC engineers in the development and evaluation feedback control and fault detection and diagnostic (FDD) algorithms. Significant literature exists on dynamic models of vapor compression systems. Much of it is restricted to air-to-air systems and few papers deal with liquid chillers. Most of existing liquid chiller models reviewed were found to use lumped capacitances for the heat exchangers, and black-box models for the compressor. Also, little or no information has been presented on execution speeds. The current work was undertaken to meet the requirement of a dynamic model of a vapor compression centrifugal chiller based on first-principles that runs at speeds close to real-time. A dynamic centrifugal water chiller model is developed and validated using experimental data. The shell-and-tube heat exchangers are modeled using a finite-volume formulation. The centrifugal compressor is developed from a combination of a simple physical model and a quasi-steady state model. Inlet guide vane capacity control is incorporated. A first principles thermostatic expansion valve is used. The model is validated using data from a 90-ton centrifugal chiller test stand, operating with R134a. Model performance during start-up and a typical load change transient is presented. The model was implemented in C++, and allows for flexibility in application to other systems of similar configuration. Also, the model is modular, allowing component models to be replaced. Model-speed to real-time ratios in the range 1.0-1.2 are achieved on a Pentium 4 1.8GHz/512MB computer.

NOMENCLATURE

Symbols

A	heat transfer area	$\dot{m}$	mass-flow rate	$\dot{V}$	volumetric flow rate
$a_0...a_4$	Constants	M	Mass	v	specific volume
$c_0...c_4$	regression coefficients	Nu	Nusselt number	W	specific polytropic work
C_p	specific heat	P	Pressure, power	y	valve lift
C	Constants	Pr	Prandtl number	α	heat transfer coefficient
D	tube diameter	$\dot{Q}$	heat transfer rate	γ	control factor
f	friction factor	Re	Reynolds number	η	polytropic efficiency
g	Accn. due to gravity	T	temperature (C)	μ	dynamic viscosity
h	specific enthalpy	u	specific internal energy	ρ	density
k	thermal conductivity, spring compliance	V	node volume (m^3)	$\dot{Q}''_r$	refrigerant heat flux

Subscripts

1	Evap exit	2	Comp exit	3	Cond exit	4	Evap inlet	b	Bulb
c	Cond	e	Evap	i	i^{th} node	t	Tube	we	Evap water
cc	Comp cooling	em	Electro-mech	in	Inlet, inner	v	Vapor, valve	wc	Cond water

INTRODUCTION

Dynamic models are crucial tools for the controls engineer in developing efficient control algorithms. Dynamic performance modeling of vapor compression systems has been of interest for well over 20 years, beginning with Dhar and Soedel [1979]. In preparation for this model development exercise, an extensive literature survey was carried out and is reported in a separate document (Bendapudi and Braun [2002]). Papers related to liquid chiller models include Sami et al [1987], Svensson [1999], Wang and Wang [2000], Browne and Bansal [2000] and Grace and Tassou [2000]. None of these models is comprehensive in that they either do not consider centrifugal compressors or they use simplified heat exchanger models that cannot adequately model large and small scale transients. Sami's model used a hermetically sealed reciprocating compressor, while Browne's dealt with screw compressors. Svensson's work presented only transients triggered by feedback control. Wang's model, which does characterize a centrifugal liquid chiller model, utilizes very simple heat exchanger models. Grace and Tassou modeled a reciprocating compressor with a shell-and-tube evaporator that operated with refrigerant flowing inside the tubes. The heat exchangers were modeled as done by MacArthur and Grald [1987]. Browne and Bansal [1998], in their compilation work on issues related to modeling of vapor compression liquid chillers, highlight the need for a liquid chiller model that incorporates detailed heat exchangers.

To summarize, it was found that no publicly available system models existed that could predict the complete dynamic performance of vapor compression centrifugal liquid chillers despite such systems being among the more popular configurations in the field.

These observations provided the motivation for defining the modeling objectives as follows:
Develop a transient model of a vapor compression centrifugal liquid chiller system that:

- is based on first principles wherever available information permits
- can capture start-up transients, as well as transients caused by feedback control
- can execute close to real-time, if not faster and
- can be used to study (in the future) the impact of common faults that occur in such systems

TEST STAND DESCRIPTION

The test stand used for the validation of the model is a 90-ton water chiller charged with R134a. The refrigeration system itself consists of a centrifugal compressor with variable inlet guide-vanes for capacity control. The heat exchangers are of shell and tube construction, with two-water passes and one refrigerant pass. The expansion valve is a cascaded device consisting of a main valve driven by a pilot valve. The compressor is powered by an electric motor. The motor and transmission are cooled by the refrigerant through a bleed line tapped off of the liquid line, as shown in Fig. 1. This refrigerant returns to the evaporator inlet. The load on the chiller system is controlled by an arrangement of heat exchangers that simulate the building load, as shown in the Fig. 2. For clarity, the pumps and valves that control the water flow rates are not shown. The load on the system can be varied by altering the temperatures of the water entering the evaporator and condenser, i.e., varying the operating conditions of these peripheral heat exchangers. An exhaustive description of the test stand and instrumentation is provided in Comstock [1999].

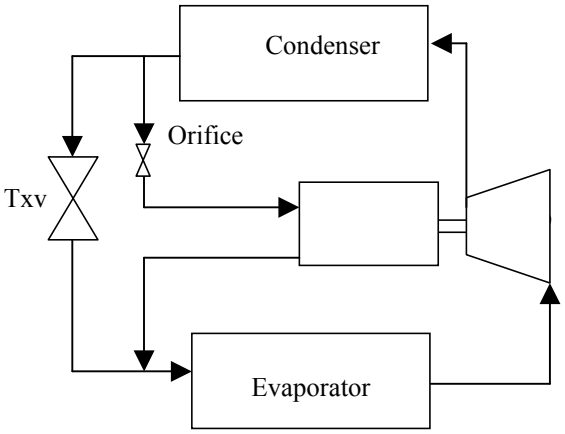

Fig. 1 Refrigerant flow paths

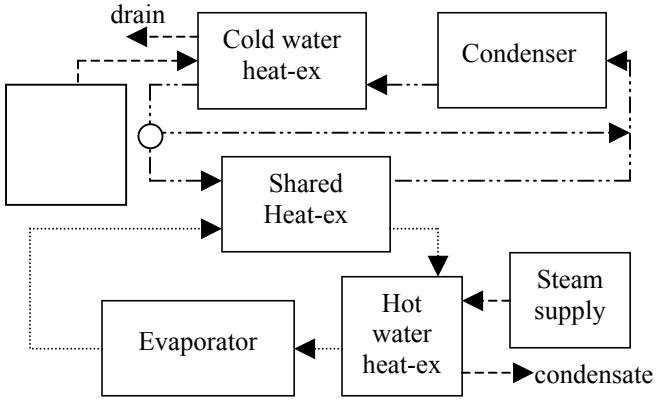

Fig. 2 Water flow paths

MODEL DESCRIPTION

For the purposes of this model, the following dynamics were considered relevant

- refrigerant re-distribution between the evaporator and condenser
- thermal capacitance of the tube-material
- thermal capacitance of the water resident inside the tubes
- thermal capacitance of the superheat sensing bulb and
- controller actuation dynamics

Other dynamics in the system include the thermal capacitances of the heat-exchanger shells and of the compressor body. These are assumed negligible at this time and may be incorporated in the future. Also ignored were the issues of oil-migration and refrigerant-oil mixing.

Heat exchanger model

The following assumptions were made in modeling both the heat-exchangers.

- One-dimensional refrigerant flow through the shell
- Pressure drops in the heat exchangers and piping are negligible
- Two-phase regions in the heat-exchanger are homogenous
- Water-flow is single-pass in both heat-exchangers
- Tube material conductance is infinite
- Shells are adiabatic
- Water in each tube is fully mixed.

The heat exchangers are modeled as described by Rossi and Braun [1999] with modifications appropriate for a shell-and-tube construction. This choice was made in the interest of fast execution times. The formulation is a linearized, finite volume approximation. The shell volume is divided into control volumes that encompass the entire shell length in the longitudinal dimension, the width of the shell in the lateral dimension and span one or more (integer number of) tube-rows in the vertical dimension.

In the general case, the refrigerant dynamics in both heat exchangers are governed by conservation of mass, energy and momentum. The assumption of zero pressure drop allows the physics to be modeled using only the mass and energy conservation equations, which for any control volume in the heat exchanger are:

$$\frac{d(\rho V)}{dt} = \dot{m}_{in} - \dot{m}_{out} \qquad \frac{d(\rho u V)}{dt} = \dot{m}_{in} h_{in} - \dot{m}_{out} h_{out} - \dot{Q}_r$$

These equations form a pair of coupled, non-linear partial differential equations. Discretizing these equations by a constant-volume approach and linearizing the coefficients, they can be re-written as a pair of coupled, ordinary linear differential equations, in which the subscript *i* refers to the *i*th control volume.

$$a_i \frac{dP}{dt} + b_i \frac{dh_i}{dt} = \dot{m}_{i-1} - \dot{m}_i \qquad c_i \frac{dP}{dt} + d_i \frac{dh_i}{dt} = \dot{m}_{i-1} h_{i-1} - \dot{m}_i h_i - \dot{Q}_{r,i}$$

The linearized coefficients are defined as:

$$a_i = V_i \left(\frac{\partial \rho}{\partial P} \right)_h \qquad b_i = V_i \left(\frac{\partial \rho}{\partial h} \right)_P \qquad c_i = V_i \left[h \left(\frac{\partial \rho}{\partial P} \right)_h - 1 \right] \qquad d_i = V_i \left[h \left(\frac{\partial \rho}{\partial h} \right)_P + \rho \right]$$

Enforced in this formulation is a form of upwinding with the refrigerant assumed to always flow in the same direction throughout the system. This is necessitated by the fact that the momentum equation is not used to establish a flow-field. However, the addition of a transient momentum equation would increase computational requirements significantly.

The above pair of equations can be compiled for all nodes in the heat exchanger and the resulting linear system of equations solved, using LU decomposition, to obtain the state derivatives and intermediate refrigerant flow rates across node boundaries.

The refrigerant exchanges heat with the tube material as well as the shell. However, the assumption of non-participative shells limits the heat transfer rate to the tube alone. This heat rate is determined from:

$$\dot{Q}_r = \alpha_r A_{out}(T_r - T_t)$$

The refrigerant-side heat transfer coefficient depends on the phase of the refrigerant and also whether it is evaporating or condensing. In single-phase conditions, as in the sub-cooled and de-superheating regions in the condenser and the super-heating region in the evaporator, this heat transfer coefficient is determined using standard correlations (Incropera and Dewitt [1996]) of the form:

$$Nu_c = C\sqrt{\mathrm{Re}}\,\mathrm{Pr}$$

The two-phase region of the evaporator is governed by boiling, and the heat transfer rate depends on the heat-flux, in the form:

$$\alpha_e = C_1 + \dot{Q}_r^{''} \Big/ C_2$$

The condensation heat transfer coefficient is determined from a standard (Dhir & Lienhard [1971]) correlation:

$$\alpha_c = 0.729\left[\frac{g\rho_l(\rho_l - \rho_v)k_l^3 h_{fg}^{'}}{\mu_l(T_{sat} - T_s)D}\right]^{\frac{1}{4}}$$

The thermal response of the tube material in either heat exchanger is determined by a lumped capacitance approach, such that:

$$M_t C_{p,t}\frac{dT_t}{dt} = \left(\dot{Q}_r - \dot{Q}_w\right)$$

The water-side heat transfer rate is determined by:

$$\dot{Q}_w = \alpha_w A_{in}\left(T_t - T_w\right)$$

where the heat transfer coefficients are determined from:

$$Nu_{we} = \frac{(f/8)(\mathrm{Re}_D - 1000)\mathrm{Pr}}{1 + 12.7(f/8)^{1/2}\left(\mathrm{Pr}^{2/3} - 1\right)}\ \text{(Gnielinski [1976])}\quad Nu_{wc} = \frac{(f/8)\mathrm{Re}_D\,\mathrm{Pr}}{1.07 + 12.7(f/8)^{1/2}\left(\mathrm{Pr}^{2/3} - 1\right)}\ \text{(Petukhov[1970])}$$

The thermal response of the water in the tubes can be similarly captured using:

$$M_w C_{p,w}\frac{dT_w}{dt} = \dot{m}_w C_{p,w}\left(T_{w,in} - T_w\right) + \dot{Q}_w$$

The above set of equations, i.e., the refrigerant mass balance, the refrigerant energy balance, the tube-material energy balance and the water energy balance, form a closed system of 4N (N being the number of control volumes in the heat exchanger) linear, first-order ordinary differential equations (for each heat exchanger) that can be integrated, given an initial condition and boundary conditions in the form of refrigerant inlet and outlet flow-rates, inlet refrigerant enthalpy and water flow rates and entering temperatures.

Compressor model

In general the time constant of the compressor's response is much smaller than that of the system. As such, the compressor can be treated as reaching steady state instantaneously and can be modeled as a quasi-steady-state device. The compression is assumed to be adiabatic and polytropic efficiency correlated. From data measured off the test stand (Comstock [1999]), the polytropic efficiency was correlated as a second order polynomial in the volumetric flow rate and polytropic work as:

$$\eta_p = a_0 + a_1\dot{V} + a_2\dot{V}^2 + a_3 W_p + a_4 W_p^2$$

This, applied to the polytropic work given by:

$$W_p = (P_c v_2 - P_e v_1)\frac{Ln[P_c/P_e]}{Ln[(P_c v_2)/(P_e v_1)]}$$

can be used to determine the motor power, using:

$$P_{motor} = \dot{m}_r \frac{W_p}{\eta_p \eta_{em}}$$

The predicted actual refrigerant flow-rate is determined by a (assumed) linear controller as

$$\dot{m}_{r,act} = \gamma.\dot{m}_{r,\max}$$

where γ is the normalized control action representative of the fractional vane-opening. This control factor can be computed from the control algorithm chosen (or available for the system being modeled) based on the error in chilled water temperature. The maximum flow rate corresponds to what the compressor would deliver if the vanes were wide open. This flow rate was developed from a first-principles model of the impeller (making approximations in geometry where information was unavailable) using the formulation developed by Braun et al [1987] and regressed as a 2nd order polynomial as:

$$\dot{m}_{r,\max} = c_0 + c_1 P_e + c_2 P_c + c_3 T_1 + c_4 P_e P_c$$

An energy balance across the compressor gives:

$$P_{motor} = \frac{\dot{m}_r (h_2 - h_1)}{\eta_{em}}$$

The above system of equations can be solved iteratively for the exit enthalpy, for given pressures, inlet enthalpy and chilled water temperature error. Knowing the pressure, the heat losses from the motor and transmission can be determined explicitly by the energy balance as:

$$\dot{Q}_{cc} = (1 - \eta_{em}) P_{motor}$$

All of this loss is assumed to be absorbed by the refrigerant bled off at the liquid line before the refrigerant is fed into the evaporator. This provides the required cooling for the motor and transmission. The electro-mechanical efficiency used above was estimated from steady-state measurements.

Valve model

The expansion across the valve is assumed isenthalpic. The device is a thermostatic expansion valve with a cross-charged superheat sensing bulb. The dynamics of the bulb are treated in a lumped capacitance form as:

$$C_b \frac{dT_b}{dt} = (T_1 - T_b)$$

where the C_b is a bulb time-constant estimated from measurements. Integrating this equation, the bulb temperature, and therefore the pressure, is determined which then acts against the evaporator pressure across the spring and controls the lift:

$$y = k_{spring} (P_b - P_e - \Delta P_{\min})$$

The ΔP_{min} accounts for the minimum superheat below which the valve remains closed. Knowing, or approximating, the dependance of flow area on the lift allows the determination of the flow rate through the valve, as:

$$\dot{m}_r = C_d A_v \sqrt{2(P_c - P_e)/v_3}$$

With the exit states from the evaporator and the condenser known, the valve equations can be solved for the flow-rate.

System model

The individual component models are combined into a system model. The system states can be integrated forward in time, given an initial condition in the form of system pressures and enthalpy distributions along the heat exchangers and inputs in the form of evaporator and condenser water temperatures and flow-rates and a chilled water set point temperature.

The compressor equations are solved first and the flow-rate and exit enthalpy are determined from current values of system pressures, evaporator exit condition and chilled water temperature error. This is followed by the valve equations from which the valve flow rate is determined, again from current system pressures and evaporator exit condition. Knowing the compressor and valve flow-rates and compressor exit enthalpy, the condenser equations are integrated forward in time by 1 sec, using externally specified water flow-rate and entering temperature. The evaporator equations are similarly integrated forward in time by 1 sec using the valve flow rate and compressor flow rates. The enthalpy of refrigerant entering the evaporator is corrected by adding the heat loss from the motor and transmission. When both the heat exchangers are solved, a new set of system pressures and enthalpy distributions are obtained, which can then be used to re-compute the compressor and valve conditions. In this manner, the cycle is repeated through start-up, steady-states and load change transients.

The heat exchanger equations are integrated forward in time using an explicit Euler method with a one-step correction. The integration time step is generally fixed, but is halved if the mass balance error across any one time step exceeds a maximum limit. This method ensures that the integration algorithm is second order accurate in time and yet avoids the iterative computations of a fully implicit scheme. At the same time, the error is kept under check when necessary. All other differential equations in the system are integrated using an explicit Euler method with fixed time steps. The compressor model is solved using a Secant method search for the exit enthalpy.

VALIDATION

The model was validated using data from a 90-ton centrifugal chiller test set-up. The chiller operates with R134a and uses water as the coolant. The model was initialized to an equilibrium condition corresponding to the system having been kept off for an extended period. The uniform pressure in the system corresponds to the saturation pressure at the evaporator water leaving temperature. The refrigerant in the evaporator is a two-phase mixture, while that in the condenser is at superheated condition at the temperature of the condenser water exit temperature. Given the total system charge, the pressure and enthalpy distribution within the heat exchangers can be uniquely identified. At this time, the system is switched on and proceeds through a start-up transient at the end of which it reaches a steady-state condition. This is followed by a sequence of 27 load changes triggered by different combinations of changes in evaporator and condenser return water temperatures and chilled water set-point temperatures (refer Comstock [1999] for the experimental data collection).

RESULTS AND DISCUSSION

Simulation results of the model compared with the measurements are shown below for the following cases:

- Start up
- A load change caused by a 2.78^{o}C drop in the chilled water set-point temperature, a 12.64^{o}C increase in evaporator water return temperature and a 1.48^{o}C increase in condenser water return temperature.

Fig. 3 shows the models ability to capture the correct steady-state conditions accurately. The controller on the test-stand restricts the motor power from exceeding a pre-set limit at high capacities. This feature in the model prevents the compressor from being able to deliver the throughput necessary to match the high capacities. This is the reason for the under-prediction in evaporator capacities at the high end.

Figs. 4-7 present the predicted system pressures and capacities match the measured responses well during start-up as well as during feedback control. The chilled water temperature quickly follows the changed set-point despite simultaneous disturbances to the evaporator and condenser return water temperatures. The faster rise rates in condenser pressure and water temperatures during start-up are believed to be a consequence of neglecting thermal masses of the shell and compressor body. This assumption deprives the refrigerant of alternate sinks (or sources) during the transient to dampen the pressure rise rate. This also partially accounts for the predicted (but not measured) transient in the evaporator water temperature during a load change (Fig. 7).

Although the evaporator pressure predicted is quite close to the measurements, it is not as well predicted as the condenser pressure. This is believed to be a consequence of approximating the expansion device model as a single thermostatic device to represent the cascaded pilot-driven main valve arrangement that exists on the system. The unaccounted non-linearities in the original arrangement and the approximated valve dimensions used in the valve model result in a different measured evaporator pressure response. A consequence of this is that the predicted superheat (not shown) also differs from the measurement.

Also observed is a variation in some steady-state motor power predictions (Figs. 8 & 9), particularly during very-low load and very-high load operation. One possible reason for this is the linear assumption made in the control action. This approach is reasonable in the mid-capacity range, but at low-loads and high loads, the flow-rate through the compressor depends non-linearly on the inlet-guide vane position. The transient response however, is independent of this and is seen to match the measured power well (Fig. 9).

Fig. 10 shows the predicted and measured sub-cooling versus time. During model execution, the total refrigerant charge required some adjustment (reduction) from the value used in the test stand during the measurements. This was necessitated by the fact that the liquid line, which contains a significant quantity of liquid refrigerant, was not modeled in any way. In addition, the assumption of homogenous two-phase conditions in the heat exchangers results in an under-prediction of refrigerant. The charge used in the system model was adjusted until the predicted

sub-cooling matched the measurements. The final adjustment amounted to reducing the manufacturer specified charge by about 8%.

Fig. 11 shows the refrigerant migration between the heat exchangers during early start-up. At start-up, the bulk of the refrigerant resides in the evaporator. On starting the compressor, the refrigerant is pumped up to the condenser and is maintained there as long as the compressor is in operation. As seen in this figure, the refrigerant movement is a transient that lasts about a 100s. The total system charge is seen to be well preserved during start-up.

CONCLUSIONS

A dynamic model of a vapor compression centrifugal liquid chiller was developed from first principles and validated. The model is found to predict start-up and feedback control transients well. The model contains adequate physical detail to allow simulation of system performance with faults introduced and is numerically stable. Further work is envisaged on improving execution speed and introduction of un-modeled non-linearities and dynamics.

REFERENCES

Bendapudi S., and Braun J.E., 2002, "A review of literature on dynamic models of vapor compression equipment", ASHRAE 1043-RP, TC 4.11.

Braun J.E., Mitchell J.W. and Klein S.A., 1987, "Models for variable-speed centrifugal chillers", ASHRAE Transactions Vol. 93, Part 1, pp. 1794-1813.

Browne M.W. and Bansal P.K., 1998, "Challenges in modeling vapor compression chillers", ASHRAE Transactions Vol. 104 Part 1, Paper No. 4141.

Browne M. and Bansal P., 2000, "Modelling of in-situ liquid chillers", Proc. 2000 International Refrigeration Conference at Purdue, pp. 425-432.

Comstock M.C., 1999, "Development of analysis tools for the evaluation of fault detection and diagnostics in chillers", MSME Thesis, Purdue University.

Dhar M. and Soedel W., 1979, "Transient analysis of a vapor compression refrigeration system.", XV International Congress of Refrigeration, Venice.

Dhir V.K. and Lienhard J.H., 1971, "Laminar film condensation on plane and axisymmetric bodies in non-uniform gravity", Journal of Heat Transfer, Vol. 93, pg. 97.

Gnielinski V., 1976, "New equation for heat and mass transfer in turbulent pipe and channel flow." International Chemical Engineering, No. 16, pp. 359-368.

Grace I.N. and Tassou S.A., 2000, "Dynamic simulation of liquid chillers", Proc. 2000 International Refrigeration Conference at Purdue, pp. 433-440.

Incropera F.P. and Dewitt D.P., 1996, "Fundamentals of heat and mass transfer", 4th Ed, John Wiley and Sons.

Petukhov B.S., Irvine T.F. and Hartnett J.P., 1970, "Advances in Heat Transfer", Vol. 6. Academic Press, NY.

Rossi T.M and Braun J.E., 1999, "A real-time transient model for air conditioners", Proc. 20th International Congress of Refrigeration, Sydney. Paper No. 743.

Sami S.M., Duong T., Mercadier Y and Galanis N., 1987, "Prediction of the transient response of heat pumps", ASHRAE Transactions, Vol. 93, pg. 471.

Svensson M.C., 1999, "Non-steady-state modeling of a water-to-water heat pump unit", Proc. 20th International Congress of Refrigeration, Sydney, Paper No. 263.

Wang H. and Wang S., 2000, "A mechanistic model of a centrifugal chiller to study hvac dynamics", Building Services Engineering Research and Technology, Volume 21(2), pp. 73-83.

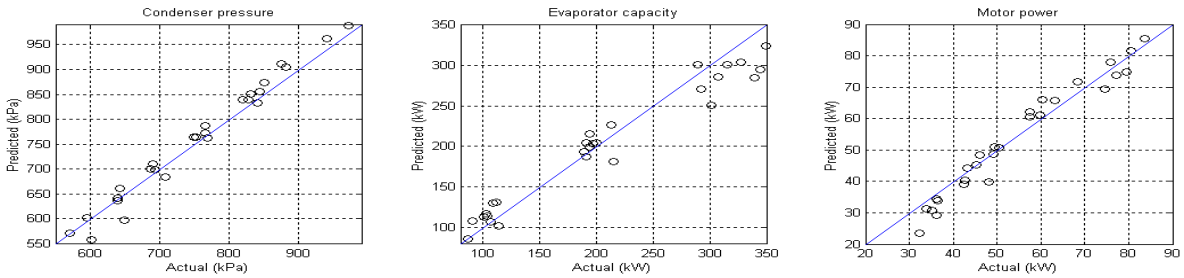

Fig. 3: Steady-state performance of the model

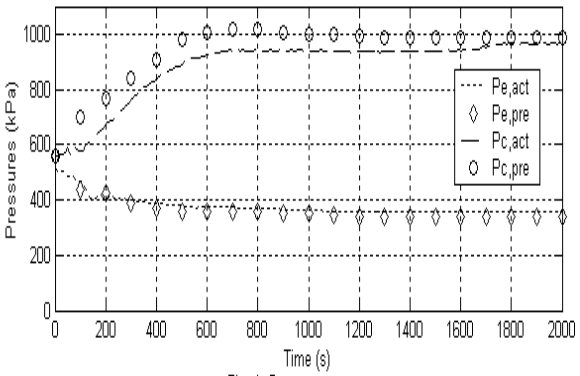

Fig. 4: Start up pressures

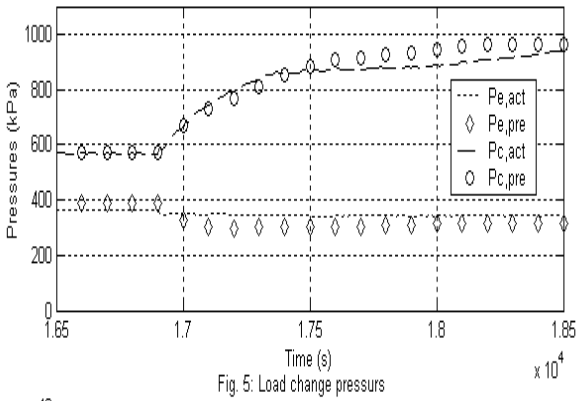

Fig. 5: Load change pressurs

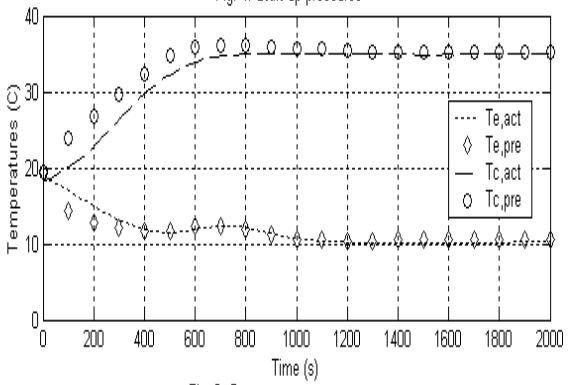

Fig. 6: Start up water temperatures

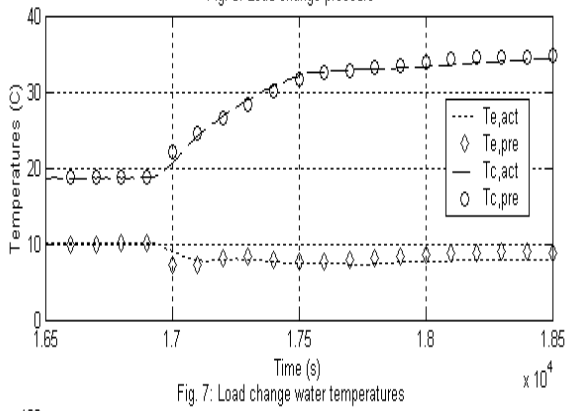

Fig. 7: Load change water temperatures

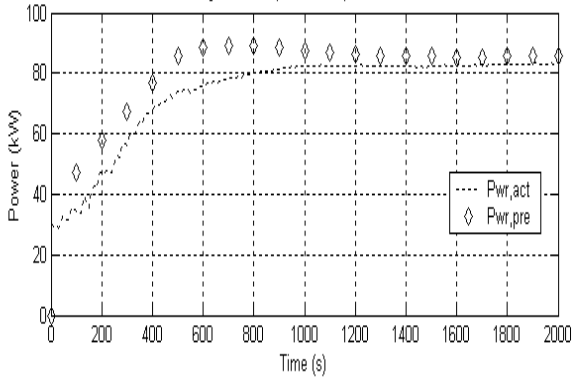

Fig. 8: Start up motor power

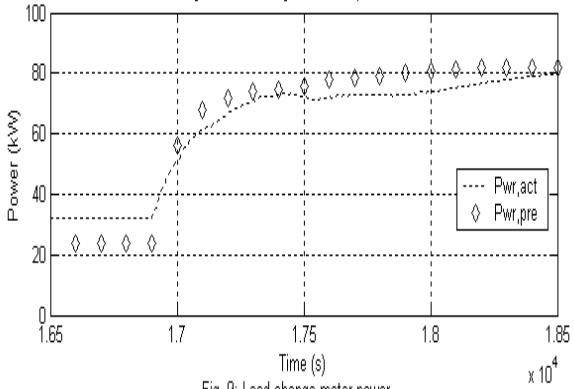

Fig. 9: Load change motor power

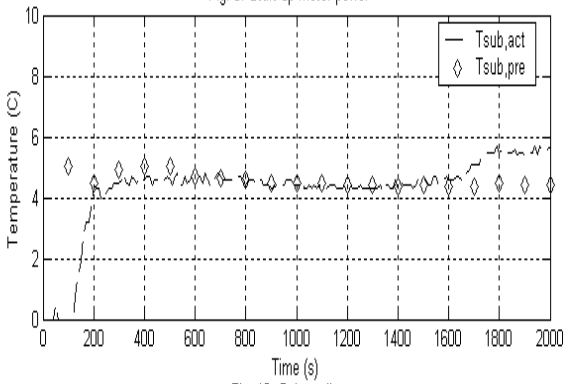

Fig. 10: Sub-cooling

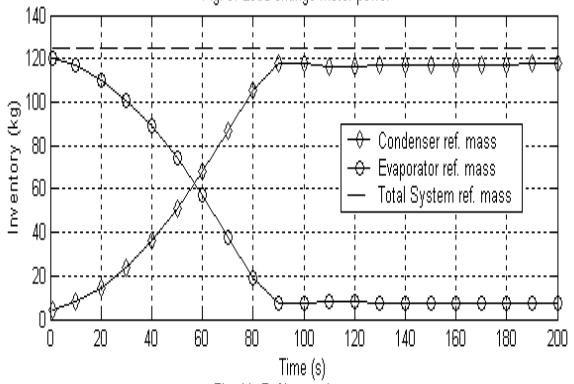

Fig. 11: Refrigerant Inventory